scientific reports

Check for updates

OPEN

Broad-spectrum antiviral activity of ebselen

Kunlakanya Jitobaom[1,2], Usa Boonyuen[3], Chompunuch Boonarkart[1,2], Thanyaporn Sirihongthong[1,2] & Prasert Auewarakul[1,2]✉

Broad-spectrum antivirals are essential for pandemic preparedness, helping reduce mortality and mitigate social disruption. Ebselen, a synthetic organoselenium compound, is under investigation for treating various conditions, including viral infections. We demonstrate that ebselen exhibits robust antiviral activity against dengue virus, Zika virus, chikungunya virus, influenza A virus, and enterovirus 71. While virus-specific mechanisms involving direct interaction with viral proteins have been reported, ebselen broad-spectrum activity suggests a common mechanism that targets host biological pathways. Ebselen inhibits inositol monophosphatase (IMPA), an enzyme critical for generating myo-inositol, a precursor for phosphatidylinositol derivatives essential to cellular processes and viral replication. Our previous study identified IMPA as a broad-spectrum antiviral target of ivermectin, and lithium, a known IMPA inhibitor, also showed antiviral effects via IMPA inhibition. We postulated that ebselen may act similarly. In this study, we confirm that IMPA silencing inhibits virus production. Notably, reduced IMPA expression partially impairs ebselen antiviral effect. Moreover, supplementation with inositol or phosphatidylinositol partially reversed ebselen activity. These results indicate that its antiviral effect is at least partly mediated through IMPA inhibition. Another IMPA inhibitor, L-690,330, also exhibited broad-spectrum antiviral activity. These findings support IMPA as a promising antiviral target and highlight ebselen potential as a broad-spectrum antiviral agent.

Keywords Ebselen, Inositol monophosphatase, Broad-spectrum antiviral, RNA viruses

Most current antiviral drugs target viral proteins and enzymes[1,2]. Because of the highly diverse nature of viruses, these drugs each usually covers only a narrow spectrum of closely related viruses. This precludes pre-development of antiviral drugs for novel and not yet known viruses. A broad-spectrum antiviral with potential to be effective for new viruses is crucial for pandemic preparedness. Although some broad-spectrum antivirals exist, there is no guarantee that they will be effective against a new pandemic virus. Availability of as many candidates with broad-spectrum antiviral activity as possible will ensure that many will be swiftly tested in clinical trials when a pandemic happens and there will be some shown to be effective.

Ebselen, a synthetic organoselenium compound that mimics the antioxidant activity of glutathione peroxidase and also exhibits anti-inflammatory and immunomodulatory properties, has been under development for various therapeutic applications[3]. It has also been investigated for its potential as a repurposed drug for viral infections. Ebselen and its derivatives have previously been identified as potent antiviral agents against severe acute respiratory syndrome coronavirus 2 (SARS-CoV-2), acting through the inhibition of the main protease (Mpro) and the papain like protease (PLpro)[4–9]. The inhibition of SARS-CoV-2 Mpro occurs through a selenation mechanism[4], where hydrolysis of the selenium-harboring compound by Mpro results in the incorporation of selenium into the Mpro catalytic dyad, rendering it inactive[10,11]. Moreover, ebselen was found to inhibit the N7-methyltransferase activity of SARS-CoV-2 nsp14 [9], which is essential for viral RNA capping[12]. Furthermore, ebselen has been previously found to inhibit human immunodeficiency virus type 1 (HIV-1), by interacting with the lens-epithelium-derived growth factor (LEDGF/p75)-binding site on HIV-1 integrase (IN), thereby disrupting viral genome integration into host cellular DNA. Additionally, screening for compounds targeting the C terminal domain of the HIV-1 capsid identified ebselen as an inhibitor of HIV-1 capsid dimerization, thus preventing viral replication[13]. In hepatitis C virus (HCV) life cycle studies, ebselen was shown to inhibit viral entry[14], and later its interaction with HCV NS3 helicase was identified, affecting viral genome replication[15]. These findings suggest that ebselen antiviral effects are mediated through direct interaction with viral proteins.

[1]Department of Microbiology, Faculty of Medicine Siriraj Hospital, Mahidol University, Bangkok 10700, Thailand. [2]Emerging Infectious Diseases Research Unit, Research Department, Faculty of Medicine Siriraj Hospital, Mahidol University, Bangkok 10700, Thailand. [3]Department of Molecular Tropical Medicine and Genetics, Faculty of Tropical Medicine, Mahidol University, Bangkok 10400, Thailand. ✉email: prasert.aue@mahidol.ac.th

Moreover, ebselen was also identified as an inhibitor of inositol monophosphatase (IMPA) through high-throughput screening aimed at finding lithium alternatives[16,17]. Lithium is a well-known IMPA inhibitor used to treat mood disorders by reducing brain levels of inositol; however, it is associated with various adverse effects. The lithium-mimetic activity of ebselen has thus been investigated for the treatment of mood disorders[3,18]. In a mouse model of bipolar disorder, ebselen demonstrated therapeutic effects via myo-inositol reduction, similar to lithium; this was confirmed by reversal upon inositol supplementation[17]. Several clinical trials are currently exploring ebselen as a treatment for various conditions, including brain injuries, hearing loss, and bipolar disorder, and have demonstrated promising safety profiles[18–20].

Inositol and its derivatives are essential for various cellular functions. Inositol is a six-carbon sugar alcohol that exists in nine stereoisomeric forms, with myo-inositol being the predominant and biologically most important form in animals. Intracellularly, myo-inositol exists in various forms, including free inositol, inositol mono- and polyphosphates, phosphatidylinositol (PI), and multiple phosphorylated derivatives of PI, known as PIPs or phosphoinositides[21]. PIPs exist in several forms, include phosphatidylinositiol-3-phosphate [PI(3)P], PI(4)P, PI(5)P, PI(3,4)P2, PI(3,5)P2, PI(4,5)P2, or PI(3,4,5)P3. Each form localizes preferentially to specific cellular membranes. For example, PI(4)P is enriched in the Golgi apparatus, PI(3)P in endosome and PI(4,5)P2 in the plasma membrane[22–24]. These distinct distributions give organelles their unique PIP compositions, effectively acting as a "zip-code system" [25]. PIPs play important roles in intracellular signaling involved in many biological processes. The different phosphate configurations on the inositol headgroup serve as docking sites for various cellular factors[25,26]. Notably, in a key signaling pathway triggered by activation of G protein-coupled receptors (GPCRs), phosphatidylinositol 4,5-bisphosphate [$PI(4,5)P_2$], which is stored in the plasma membrane, is hydrolyzed by phospholipase C into diacylglycerol and inositol trisphosphate, both of which function as secondary messengers[27,28]. Although PIPs constitute only a minor fraction of total membrane phospholipids, they are crucial regulators of membrane organization[29].

Inositol can be obtained through dietary intake or *de novo* synthesized from glucose. Cellular uptake of inositol occurs via two major types of transporters: (1) sodium ion-coupled inositol transporters and (2) proton-coupled inositol symporters[30]. For *de novo* biosynthesis, glucose-6-phosphate is first converted into inositol-3-phosphate by inositol-3-phosphate synthase, and then to inositol by IMPA[31]. IMPA is also responsible for the recycling of inositol released from PI(4,5)P2, which is metabolized into IP3, contributing to a complex signaling network involving various inositol phosphates[31]. In mammals, two distinct isoforms of IMPA exist, IMPA1 and IMPA2, with different expression patterns across tissues[32].

As viruses rely on host cell machinery, PIPs have been shown to be essential for the replication of several viruses. It is believed that PIPs serve as docking sites for viral proteins on replication organelles (ROs)[26]. Phosphatidylinositol kinases (PIKs), which phosphorylate phosphatidylinositol to generate distinct PIP species, are therefore crucial in this context. Inhibitors of PIKs have demonstrated antiviral activity[26,31]. Additionally, PI3Ks and PI4Ks, in particular, are targets for both anticancer and antiviral drug development[33,34]. However, different viruses, as well as different genotypes of the same virus, utilize and manipulate distinct PIKs to support their replication[26], making the development of broad-spectrum PIK inhibitors as antiviral agents particularly challenging.

Our previous study demonstrated that inhibition of IMPA by ivermectin and lithium reduced cellular myo-inositol and its derivatives, which are essential for viral replication, thereby inhibiting the production of multiple viruses[35]. These findings highlight the importance of IMPA as an antiviral target for a range of viruses. Due to its upstream role in the biosynthesis of all PIP species, IMPA inhibition is expected to reduce the levels of all PIPs, thereby disrupting their downstream signaling functions, including those required for viral replication. Taken together with the IMPA-inhibitory activity of ebselen, it is postulated that ebselen may exert antiviral effects not only through direct interaction with viral proteins and immunomodulation, but also via IMPA inhibition, thereby conferring broader antiviral activity. To expand the repertoire of potential antiviral agents and further validate IMPA as a therapeutic target, we investigated the antiviral activities of ebselen and L-690,330, another well-characterized IMPA inhibitor.

Results

Ebselen inhibits IMPA activity and reduces myo-inositol levels. An *in vitro* enzymatic assay of IMPA activity was conducted using recombinant human inositol monophosphatase 1 (IMPA1) treated with various concentrations of ebselen. IMPA1 catalyzes the conversion of inositol monophosphate into *myo*-inositol and a phosphate group. Following the enzymatic reaction, the amount of released phosphate was measured. The resulting dose-response curve illustrates IMPA1 activity normalized to the untreated control. Ebselen demonstrated IMPA1 inhibition, reducing enzyme activity with an IC_{50} of 0.95 μM. Lithium, a well-known IMPA inhibitor, was used as a positive control for IMPA inhibition in this study, with LiCl serving as the form used in the experiments. Upon treatment with LiCl, IMPA activity was inhibited with an IC_{50} of 250 μM (Fig. 1A). Moreover, cells treated with 30 mM LiCl or 25 μM ebselen showed a significant reduction in myo-inositol levels ($p = 0.03$ and 0.01, respectively) (Fig. 1B).

Antiviral activity of ebselen against various RNA viruses

The antiviral activity of ebselen was demonstrated against various RNA virus genera, including flaviviruses, alphaviruses, enteroviruses, and orthomyxoviruses. The IC_{50} values of ebselen were 16.90, 7.40, 2.02, 7.10, and 1.57 μM for dengue virus serotype 2 (DENV-2), Zika virus (ZIKV), chikungunya virus (CHIKV), enterovirus 71 (EV71), and influenza A virus (IAV), respectively (Fig. 2). Furthermore, selectivity index (SI) values were calculated, indicating favorable therapeutic windows (Table 1). Additionally, some viruses were selected and tested with L-690,330, an IMPA inhibitor, to confirm that inhibition of IMPA affects viral replication. L-690,330 also exhibited antiviral activity against various RNA viruses at higher concentrations. The IC_{50} values of

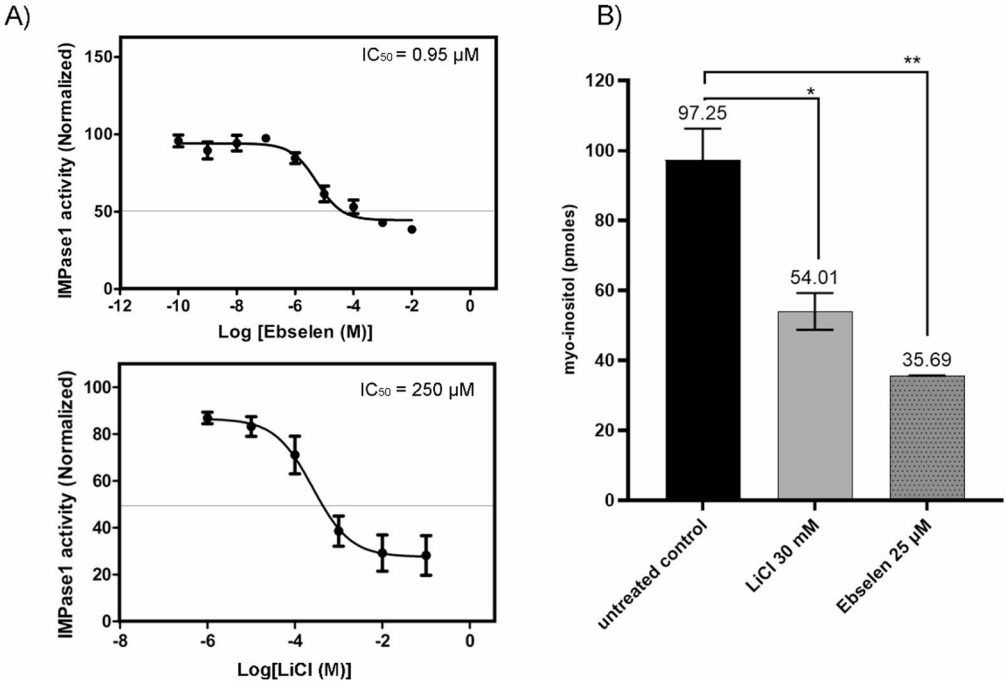

Fig. 1. Ebselen inhibits IMPA activity and reduces myo-inositol levels. (**A**) In the in vitro enzymatic assay of IMPA activity, a recombinant human inositol monophosphatase 1 (IMPA1) was treated with various concentrations of ebselen or LiCl. The amount of released phosphate was determined using a phosphate assay kit. IMPA1 activity was then normalized against an untreated control. (**B**) Additionally, the cells were treated with ebselen (25 µM) or LiCl (30 mM) for 2 days. Subsequently, the myo-inositol content in each sample (1×10^6 cells) was quantified using a myo-inositol assay kit. Differences between treated samples and the untreated control were compared pairwise using the independent samples t-test (*$p \leq 0.05$; **$p \leq 0.01$).

L-690,330 were 832.5, 830.1, 548.3, and 642.4 µM for DENV, ZIKV, CHIKV, and EV71, respectively (Fig. 3). The IC_{50}, CC_{50}, and SI values of ebselen and L-690,330 are summarized in Table 1.

Reversal of ebselen antiviral activity by inositol and phosphatidylinositol (PI)

To demonstrate that the antiviral mechanisms of ebselen can be mediated through IMPA inhibition, cells were infected with various viruses and treated with ebselen in the presence of inositol or PI at varying concentrations (Figs. 4 and 5). To assess the reversal of ebselen antiviral activity using inositol, an increase in virus production was observed in cells treated with ebselen combined with 5 mM or 10 mM inositol during DENV-2 infection (Fig. 4A). A significant increase in virus production was observed in cells treated with 10 mM inositol alone compared to the untreated control ($p = 0.003$), and in cells treated with a combination of inositol and ebselen at concentrations of 8.5 and 34 µM compared to cells treated with ebselen alone ($p = 0.043$ and 0.001). At 17 µM ebselen, the combination with 10 mM inositol resulted in relatively higher virus production compared to cells treated with ebselen alone. Similar results were observed for ZIKV (Fig. 4B), EV71(Fig. 4C), and IAV (Fig. 4E), although with varying levels of virus production restoration. However, during CHIKV infection, virus production remained unchanged or slightly increased in treatments combining ebselen with 5 or 10 mM inositol.

The partial reversal of ebselen antiviral activity using PI was also observed in DENV-2, ZIKV, EV71, and CHIKV-infected cells (Fig. 5). A significant increase was observed in the cells treated with a mixture of ebselen and 1.25–2.5 µg/ml PI at certain ebselen concentrations compared to those treated with ebselen alone. However, for EV71, virus production remained unchanged or slightly increased in treatments combining ebselen with 1.25–2.5 µg/ml PI. Cell viability of cells treated with the mixtures of ebselen and inositol, or ebselen and PI, is shown in Supplementary Fig. 1. Additionally, PI(4)P, one of the PIPs often implicated in the viral replication processes of certain viruses, exhibited increased levels following the addition of inositol (Supplementary Fig. 2). This suggests that the added inositol is capable of enhancing PIP generation.

IMPA1 silencing inhibits virus production, and reduced IMPA1 expression partially impairs ebselen antiviral effect

To confirm that the antiviral effects are mediated through IMPA1 inhibition, IMPA1 silencing was performed in imHC cells. The cells were transfected with siRNA targeting IMPA1 (si_IMPA1) or an irrelevant siRNA (si_irrelevant) as a non-targeting control. Following IMPA1 silencing, the cells were subsequently infected with DENV-2. Virus production and protein expression levels were then assessed (Fig. 6). Full membrane images from the western blot analysis are provided in the Supplementary Materials. In Fig. 6A, a significantly lower virus titer was observed in si_IMPA1-silenced cells compared to the non-targeting control ($p = 0.0001$). However, the

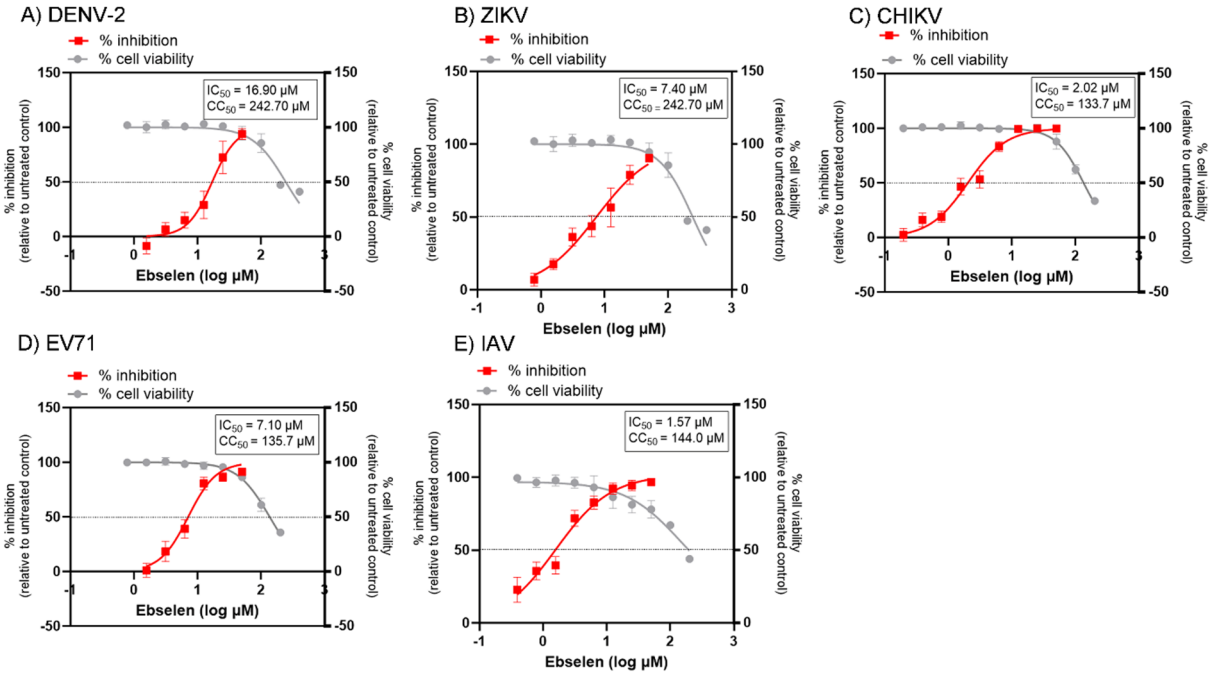

Fig. 2. Antiviral activity of ebselen against various RNA viruses. The imHC cells were infected with DENV-2 (**A**) or ZIKV (**B**) at an MOI of 1. Vero cells were infected with CHIKV (**C**), EV71 (**D**), or IAV (**E**) at MOIs of 0.0025, 0.02, and 1, respectively. Following viral adsorption, the cells were maintained in media containing various concentrations of ebselen. Virus supernatants were collected, followed by viral titer determination. The percent inhibition was calculated relative to the virus titer of the infected untreated control. Each experiment was performed in triplicate.

Chemicals	Cells	Viruses	IC_{50} (μM)	CC_{50} (μM)	Selectivity index
Ebselen	imHC	DENV-2	16.90	242.70	14.36
		ZIKV	7.40		32.80
	Vero	CHIKV	2.02	133.70	66.19
		EV71	7.10	135.70	19.11
		IAV H1N1 (2009)	1.57	144.00	91.72
L-690,330	imHC	DENV-2	832.50	3359.00	4.03
		ZIKV	830.10		4.05
	Vero	CHIKV	548.30	2081.00	3.80
		EV71	642.40		3.24

Table 1. Antiviral activity of Ebselen and L-690,330 against various RNA viruses.

virus titer in IMPA1-silenced cells treated with ebselen was significantly higher than that in the non-targeting control ($p = 0.003$), indicating a decrease inhibitory effect of ebselen, approximately a 16% reduction, in si_IMPA1-silenced cells.

Figure 6B and C show a reduction in IMPA1 expression following si_IMPA1 transfection compared to non-targeting siRNA transfection. The relative IMPA1 expression levels are plotted in Fig. 6D, demonstrating consistently and significantly reduced IMPA1 levels across mock-infected, DENV-2-infected, and ebselen-treated conditions ($p = 0.01$, 0.045, and 0.014, respectively). Additionally, no significant difference in IMPA1 levels was observed between mock- and DENV-2-infected cells ($p = 0.613$).

A reduction in DENV-2 NS1 expression was observed following si_IMPA1 silencing (Fig. 6B); however, it was not significantly different from that in the non-targeting control ($p = 0.227$) (Fig. 6E). Similarly, ebselen-treated infected non-targeting control cells also showed a lower level of DENV-2 NS1 expression ($p = 0.068$) (Fig. 6C). However, DENV-2 NS1 expression in IMPA1-silenced cells treated with ebselen was higher than that in the non-targeting control ($p = 0.21$), indicating a decreased inhibitory effect of ebselen, which corresponds to the virus production shown in Fig. 6A.

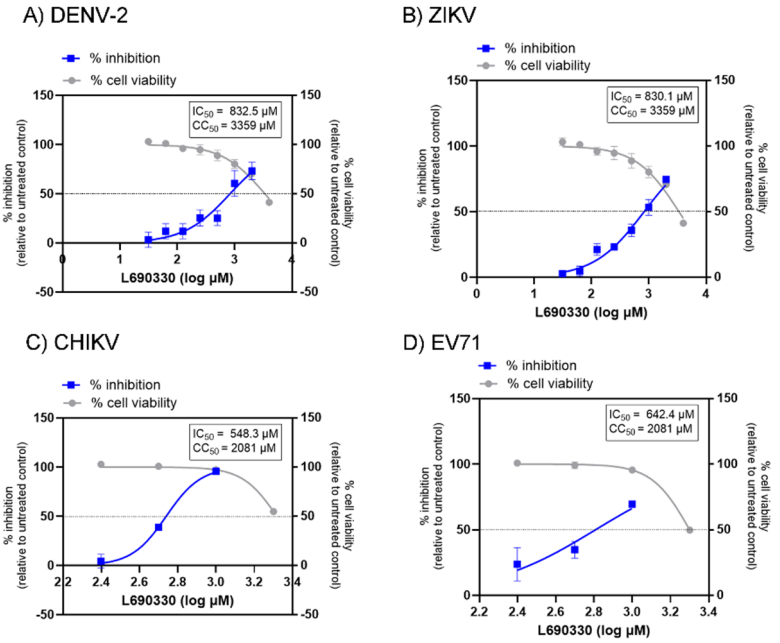

Fig. 3. L690330 inhibits IMPA activity and reduce virus production. Antiviral activity of L690,330 against various RNA viruses. The imHC cells were infected with DENV-2 (**A**) or ZIKV (**B**) at an MOI of 1. Vero cells were infected with CHIKV (**C**) or EV71 (**D**) at MOI of 0.0025 and 0.02, respectively. Following viral adsorption, the cells were maintained in media containing various concentrations of L-690,330. The viral supernatants of virus were collected, followed by viral titer determination. The percent inhibition was calculated relative to the virus titer of the infected untreated control. Each experiment was performed in triplicate.

Ebselen inhibits PI(4)P generation and virus production

Ebselen inhibits IMPA activity, leading to a reduction in myo-inositol, a precursor for PI and PIP biosynthesis. Among these, PI4Ks and their product, PI(4)P, have been identified as critical for the replication of certain viruses. A reduction in PI(4)P may therefore impair viral replication. To explore this, PI(4)P expression was examined following ebselen treatment, using ZIKV infection as a model, since ZIKV depends on PI4K and PI(4)P for its replication[36].

Figure 7A shows increased PI(4)P expression in ZIKV-NS1-positive cells, whereas ebselen treatment led to a reduction in both PI(4)P levels and ZIKV-NS1 protein expression. This corresponded to the frequency of pixel intensity levels of PI(4)P (Fig. 7B). Ebselen treatment demonstrated a lower frequency of high pixel intensity levels, suggesting a reduction in PI(4)P levels. In contrast, ZIKV-infected cells exhibited a higher frequency of high pixel intensity levels, indicating an increase in PI(4)P levels.

Discussions

Ebselen exhibits antiviral activity through multiple mechanisms. In addition to directly interacting with viral proteins, ebselen also protects host cells via its antioxidant and anti-inflammatory properties[3]. During IAV infection, increased lung oxidative stress and inflammation are common consequences that can exacerbate chronic obstructive pulmonary disease (COPD). Ebselen has been shown to reduce pro-inflammatory cytokines and chemokines induced by IAV infection in mice[37], alleviating pulmonary inflammation by inhibiting TNF-α and IL-1β, potent neutrophil-recruiting mediators and inducers of ICAM-1[38,39]. ICAM-1 is a cell surface glycoprotein upregulated in response to inflammatory stimuli.

Ebselen also shows protective effects during ZIKV infection, virions are detectable in the seminal fluid of infected hosts, facilitating sexual transmission. ZIKV induces pathogenesis in the male reproductive system of mice[40]. Ebselen has been found to reduce testicular oxidative stress and pro-inflammatory responses in mice, thereby preventing testicular pathogenesis and limiting ZIKV sexual transmission[41]. Additionally, ebselen has demonstrated antiviral activity against human herpesvirus type 1 (HHV-1) and encephalomyocarditis virus (EMCV), but not against vesicular stomatitis virus (VSV)[42].

Since ebselen has similarly been found to inhibit IMPA activity, like lithium and ivermectin, it may exert its antiviral effects through this pathway as well. Inhibition of IMPA has been identified as a broad-spectrum antiviral target of ivermectin[35]. Notably, lithium, a well-known IMPA inhibitor, has also demonstrated antiviral activity against various viruses, including DENV-2[35], coxsackievirus B3 (CVB3)[43], severe acute respiratory syndrome coronavirus 2 (SARS-CoV-2)[44], avian coronavirus infectious bronchitis virus[45], porcine reproductive and respiratory syndrome virus (PRRSV)[46], human immunodeficiency virus[47], and herpes simplex virus[48]. Importantly, evidence from DENV-2 infection study shows that lithium antiviral activity can be reversed by

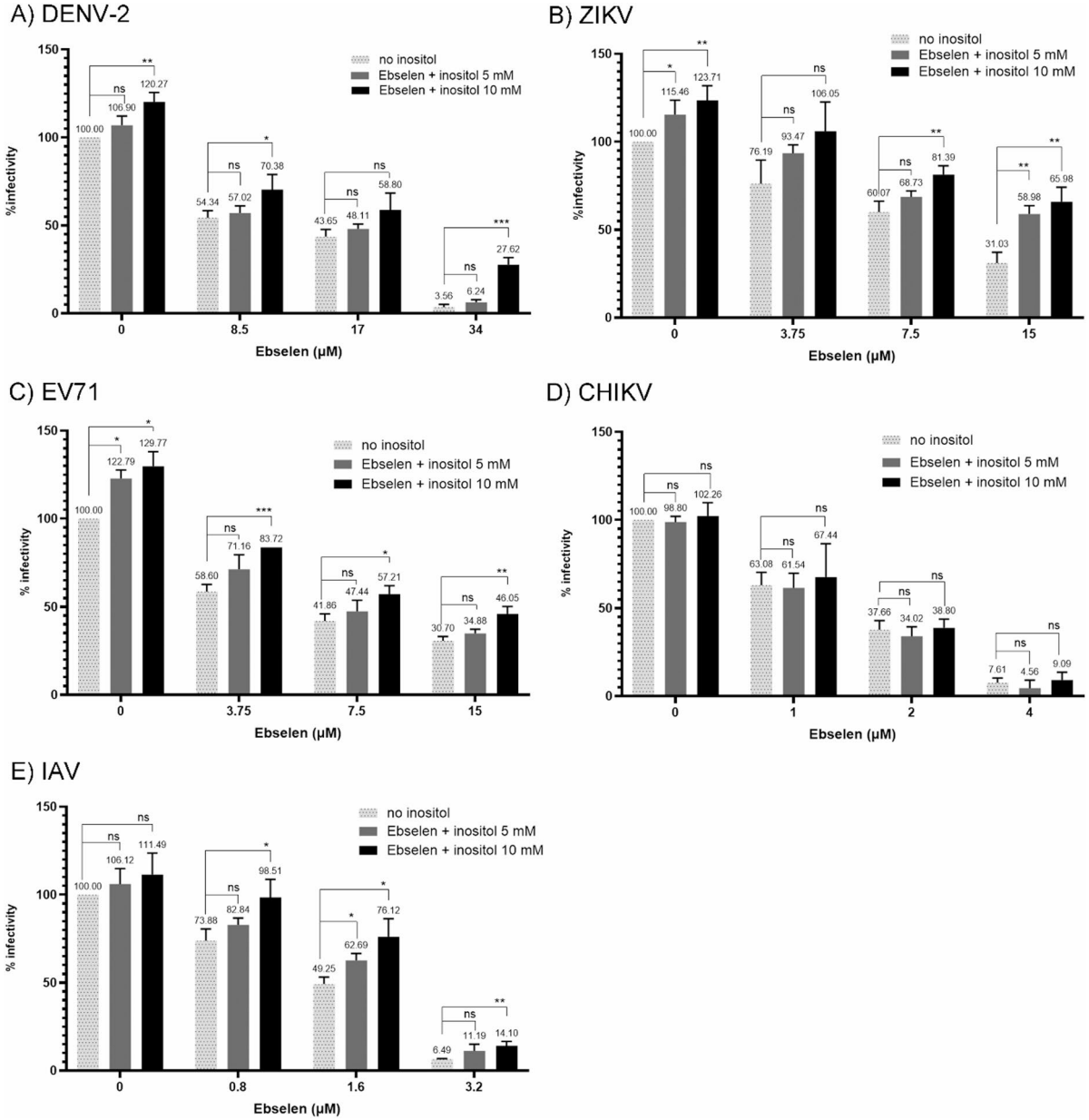

Fig. 4. Reversion of ebselen antiviral activity by inositol. The imHC cells were infected with DENV-2 (**A**) or ZIKV (**B**) at an MOI of 1, and Vero cells were infected with EV71 (**C**), CHIKV (**D**), or IAV (**E**) at an MOI of 0.02, 0.0025, and 1, respectively. After the virus inoculum was discarded, the cells were maintained in media containing various concentrations of ebselen, inositol, a combination of ebselen and inositol, or 0.5% DMSO as an untreated control. The viral supernatants of CHIKV were collected at 24 hpi, while those of DENV, ZIKV, EV71, and IAV were collected at 48 hpi. The data are presented as the mean of triplicate experiments, and error bars represent the standard deviation. The comparisons between two groups were performed using the independent samples t-test: ebselen alone vs. ebselen with 5 mM inositol, and ebselen alone vs. ebselen with 10 mM inositol (*$p \leq 0.05$; **$p \leq 0.01$; ***$p \leq 0.001$; ns = non-significant difference).

inositol supplementation, suggesting that IMPA inhibition is one of the key mechanisms through which lithium exerts its antiviral effects[35].

Additionally, beyond IMPA inhibition, lithium has been shown to act through additional antiviral pathways. During PRRSV infection, it induces the antiviral cytokine TNF-α and inhibits viral attachment and entry[46]. In CVB3 infection, lithium suppresses viral replication by inhibiting virus-induced apoptosis[43]. Furthermore, lithium has demonstrated protective effects against SARS-CoV-2 pathogenesis by promoting membrane depolarization, which suppresses the cytokine storm via inhibition of the NLRP3 inflammasome[44].

In this study, we demonstrated that ebselen inhibits IMPA activity using an in vitro enzymatic assay with recombinant IMPA1. Similar results were observed regarding the reduction of cellular myo-inositol levels when cells were treated with ebselen. The antiviral activities of ebselen and another known IMPA inhibitor, L-690,330,

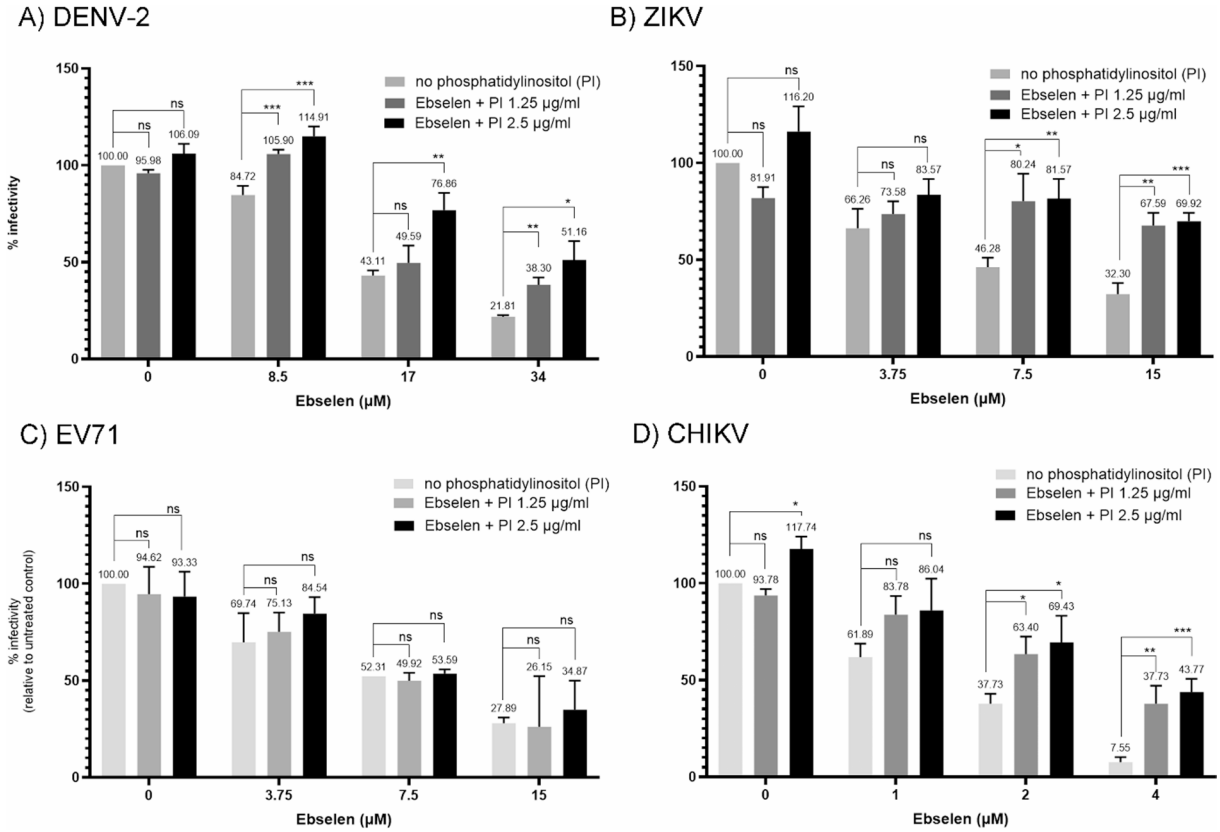

Fig. 5. Reversion of ebselen antiviral activity by phosphatidylinositol (PI). The imHC cells were infected with DENV-2 (**A**) or ZIKV (**B**) at an MOI of 1, and Vero cells were infected with EV71 (**C**) or CHIKV (**D**) at an MOI of 0.02 and 0.0025, respectively. After the virus inoculum was discarded, the cells were maintained in media containing various concentrations of ebselen, PI, a combination of ebselen and PI, or 0.5% DMSO as an untreated control. The viral supernatants of CHIKV were collected at 24 hpi, while those of DENV, ZIKV, and EV71 were collected at 48 hpi, followed by viral titer determination. The data are presented as the mean of triplicate experiments, and error bars represent the standard deviation. The differences between two groups were assessed using the independent samples t-test: ebselen alone vs. ebselen with 1.25 µg/ml PI, and ebselen alone vs. ebselen with 2.5 µg/ml PI (*$p \leq 0.05$; **$p \leq 0.01$; ***$p \leq 0.001$; ns = non-significant difference).

were evaluated against various RNA viruses. Ebselen demonstrated potent antiviral activity against DENV-2, ZIKV, CHIKV, EV71, and IAV at low micromolar concentrations, whereas L-690,330 exhibited antiviral effects only at much higher micromolar concentrations.

The viral inhibitory effect of L-690,330 suggests that IMPA inhibition might affect viral replication, despite its high IC_{50} values. These elevated IC_{50} values may be attributable to limited cell membrane permeability. L-690,330 is a competitive inhibitor of IMPA, with reported inhibition constant (Ki) values of 0.27 and 0.19 µM for recombinant human and bovine IMPA, respectively, and 0.30 and 0.42 µM for IMPA isolated from human and bovine frontal cortex[49]. Additionally, potent IMPA inhibition was observed with an IC_{50} value of 1.3 µM when using IMPA isolated from a human cerebrospinal fluid sample[50]. However, its bisphosphonate structure, comprising two phosphonate groups, results in a highly polar, polyanionic configuration that limits cellular uptake and reduces effectiveness against non-bone target cells. The three-dimensional structure of bisphosphonates enables binding to divalent metal ions such as Ca^{2+}, Mg^{2+}, and Fe^{2+}. The high avidity for Ca^{2+} ion serves as the basis for the bone-targeting properties of bisphosphonates[51,52]. Consistent with this, treatment of CHO cells with L-690,330 required a high concentration of 10 mM and achieved only 40% of the inhibitory effect observed with LiCl at the same dose. This contrasts with in vitro assays, where L-690,330 demonstrated approximately a thousand-fold greater potency than lithium[49]. To enhance intracellular delivery of L-690,330, prodrug strategies have been explored. One such approach involves the tetrapivaloyloxymethyl ester prodrug, L-690,488[53].

To demonstrate that ebselen also mediates its antiviral effects through IMPA, the reversal of ebselen antiviral activity was assessed by supplementing cells with either inositol or phosphatidylinositol. The results showed that both molecules partially restored virus production, indicating that ebselen may mediate its antiviral effects through IMPA inhibition. This partial restoration also suggests that ebselen exerts its antiviral activity through multiple mechanisms, as previously described. Therefore, supplementation with inositol or phosphatidylinositol alone cannot fully reverse its antiviral effects. A clear example is seen in the reversal experiments with CHIKV

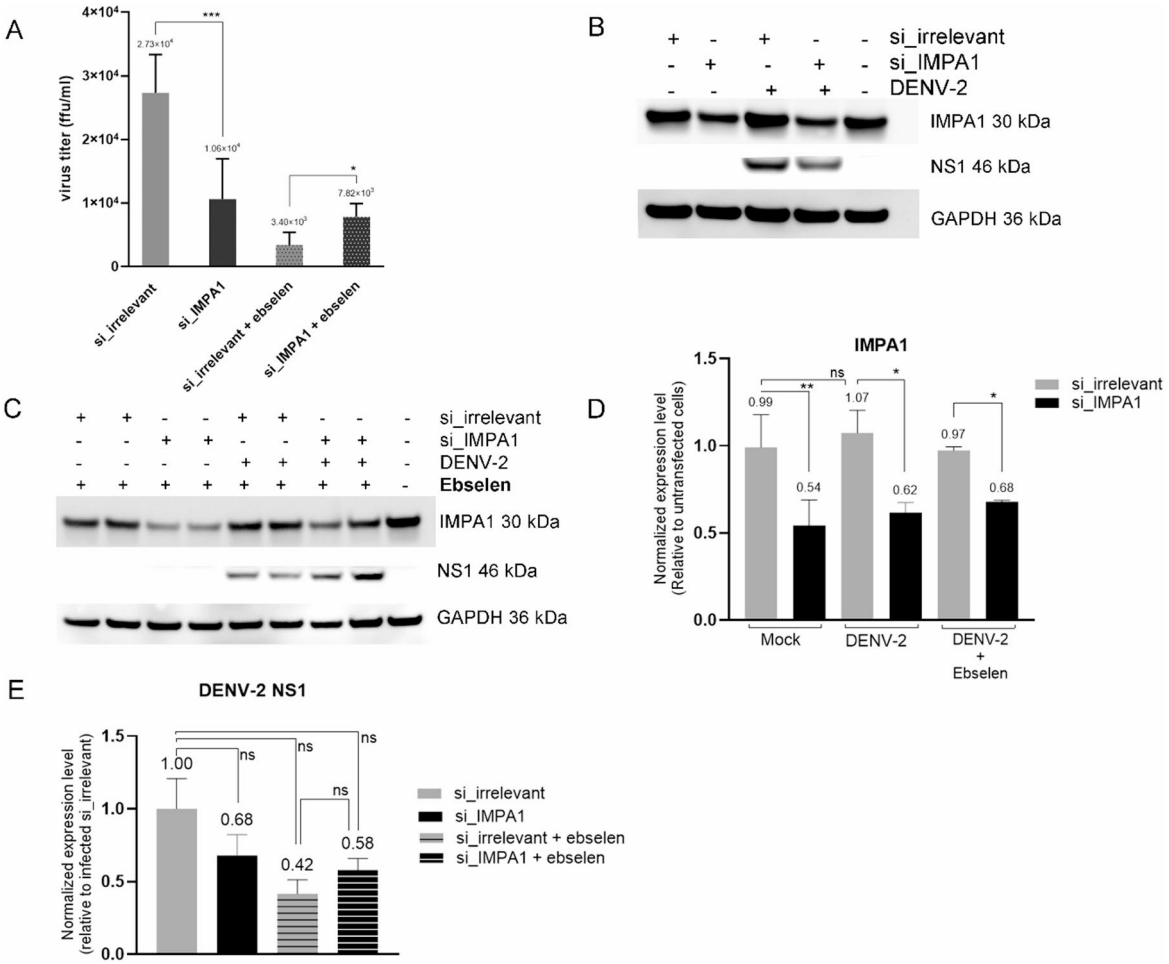

Fig. 6. **IMPA1 silencing inhibits virus production, and reduced IMPA1 expression partially impairs ebselen antiviral effect**. imHC cells were seeded in a 24-well plate at a density of 6.5 × 105 cells/well. The following day, cells were transfected with siRNA targeting IMPA1 (si_IMPA1) or a non-targeting control siRNA (si_irrelevant). Two days post-transfection, cells were either mock-infected or infected with DENV-2 at a multiplicity of infection (MOI) of 2. After removal of the viral inoculum, cells were maintained in media with or without 20 µM ebselen for 24 h. Viral supernatants were collected for virus titer quantification, and cells were harvested for protein expression analysis via western blotting. (**A**) shows the virus titer of DENV-2 in infected cells transfected with either si_irrelevant or si_IMPA1, and treated with or without ebselen. (**B**) and (**C**) display representative protein bands for IMPA1, DENV-2 NS1, and GAPDH. Protein band intensities were quantified, normalized to GAPDH expression levels, and plotted as graphs: (**D**) relative IMPA1 expression levels and (E) relative DENV-2 NS1 expression levels. Data are presented as the mean of duplicate experiments. The differences between two groups were assessed using the independent samples t-test (*$p \leq 0.05$; **$p \leq 0.01$; $p \leq 0.001$; ns = non-significant).

and EV71, where the addition of inositol or phosphatidylinositol only minimally restored virus production inhibited by ebselen (Figs. 4D and 5C).

Specifically, we demonstrated that silencing IMPA1 expression reduces virus production, indicating that IMPA1 can be antiviral target. Notably, impaired IMPA1 expression affects the antiviral effects of ebselen, as partially restored virus production and reduced inhibitory effects were observed in IMPA1-silenced cells treated with ebselen. These results suggest that the antiviral activity of ebselen is at least partly mediated through IMPA1 inhibition.

Moreover, the reduction of cellular myo-inositol levels impacts the subsequent biosynthesis of PIPs. In this study, ZIKV infection was used as a model to investigate the consequences of reduced myo-inositol levels on PIP biosynthesis and viral replication. PI(4)P is enriched in ZIKV replication organelles (ROs), which localize to the endoplasmic reticulum (ER) membrane. The positively charged residue R31 of the viral protein NS1 binds to negatively charged lipids such as PI(4)P, and this interaction plays a role in RO formation[36]. A reduction in PI(4)P levels upon ebselen treatment was observed, along with decreased ZIKV production. ZIKV targets the PI4K type III β isoform to enrich PI(4)P in its ROs[54]. The enriched PI(4)P increases the negative charge of the lipid bilayer, facilitating interaction between the ZIKV NS1 protein and the ER membrane. A previous study

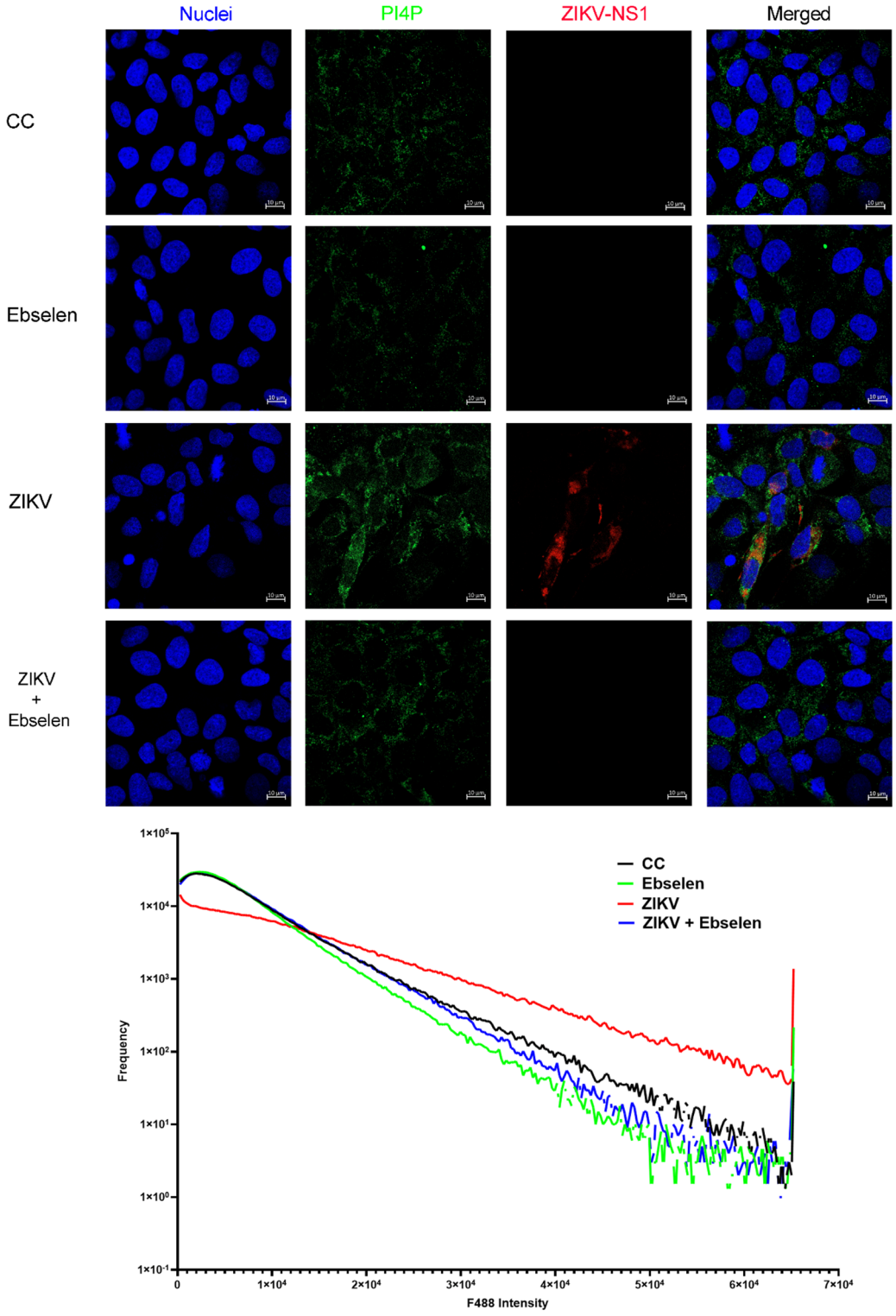

Fig. 7. PI4P and ZIKV-NS1 expression in imHC cells treated with ebselen. (**A**) The imHC cells were seeded onto 24-well plates with coverslips. The cells were either mock-infected or infected with ZIKV at an MOI of 1 for 2 h. After the removal of the virus inoculum, the cells were maintained in 2% FBS media containing ebselen or 0.5% DMSO as the untreated cell control (CC). The cells were fixed at 48 hpi and probed with a mouse anti-PI(4)P IgM antibody and a rabbit anti-ZIKV-NS1 IgG antibody. Subsequently, the cells were probed with secondary antibody-conjugated fluorescence dye and Hoechst dye for nuclear staining. Images were captured using a confocal microscope, with blue representing nuclei, green representing PI(4)P, and red representing ZIKV-NS1. The last panel shows merged images. Scale bar, 10 µm. (**B**) PI(4)P expression levels were assessed using the confocal microscope software, ZEN 3.5 (Blue Edition), to analyze the frequency of pixel intensity levels of PI(4)P (Alexa Fluor 488 dye). A graph was plotted to illustrate the relationship between pixel intensity levels and frequency

demonstrated that dephosphorylation of PI(4)P by the phosphatase Sac1 disrupts NS1-induced ER membrane remodeling and impairs ZIKV replication[36].

Ebselen demonstrates antiviral activity against various viruses with a favorable selectivity index; however, this study was limited to *in vitro* investigations involving only RNA viruses. Additionally, the antiviral properties of ebselen derivatives have been explored to improve efficacy and minimize toxicity[6,9,55]. L-690,330 also exhibits antiviral activity against various RNA viruses, but with high IC_{50} values and a low selectivity index, suggesting a narrow therapeutic window and increased cytotoxicity, making it unsuitable as a drug candidate. Ebselen potent antiviral activity is exerted through multiple mechanisms. This study reveals an additional antiviral mechanism mediated through IMPA inhibition. Given the upstream role of IMPA, its inhibition could affect the biosynthesis of phosphoinositides (PIPs), including those required by viruses, regardless of the specific PIP or phosphoinositide kinase (PIK) manipulation strategies employed by different viruses. This highlights IMPA inhibition as a promising broad-spectrum antiviral strategy that may be effective against a wide range of viral pathogens.

Methods

Chemicals

Ebselen (also known as PZ51, HY-13750; MedChemExpress (MCE)) was prepared at a concentration of 100 mM in DMSO (Sigma). Inositol (HY-B1411, MCE), L-690,330 (HY-101075, MCE), and LiCl (L9650, Sigma) were prepared at concentrations of 200 mM, 100 mM, and 3 M, respectively, in water. The solutions were stored at − 80 °C, except the LiCl solution, which was stored at room temperature (RT).

Cells

C6/36 cells (CRL-1660, ATCC) were cultivated in Leibovitz's L-15 medium (L-15, Gibco) supplemented with 10% heat-inactivated FBS and incubated at 28 °C. Vero cells (Vero CCL-81, ATCC) were cultivated in the Minimum Essential Medium (MEM/EBSS; SH30024.02, HyClone) supplemented with 10% heat-inactivated FBS. Madin-Darby Canine Kidney (MDCK; CCL-34, ATCC) cells were cultivated in MEM (Gibco) supplemented with 10% heat-inactivated FBS. Huh-7 was cultivated in high glucose Dulbecco's Modified Eagle Medium (DMEM, SH30285.02, HyClone) supplemented with 10% heat-inactivated FBS. Immortalized human hepatocyte cells (imHC) were cultivated in DMEM/F12 at a ratio of 1:1 (SH30023.02, HyClone) supplemented with 10% heat-inactivated fetal bovine serum (FBS). These cell lines were incubated at 37 °C with 5% CO_2.

Viruses

Dengue virus serotype 2 (DENV-2) strain 16,681, the Asian zika virus (ZIKV) strain (MU-DMSC-4/2017, accession number: MT377495)[56], and chikungunya virus (CHIKV) were propagated in C6/36 cells. Virus supernatants were collected at 5 days post-infection (dpi) for DENV-2, and at 7 dpi for ZIKV and CHIKV. Enterovirus 71 (EV71) subgenotype C4[57] was propagated in Vero cells. Influenza A virus (IAV) A/Nonthaburi/102/2009(H1N1) was propagated in MDCK cells. Virus supernatants of EV71 and IAV were collected at 3 dpi., then centrifuged to remove cell debris, aliquoted, and stored at − 80 °C.

Cell viability assay

The procedure for cell viability assay was described elsewhere[35]. Cells were seeded in 96-well plates at a density of 2×10^4 cells per well. The following day, cells were treated with twofold serial dilutions of ebselen or L690,330 in 2% FBS media for 48 h. Cells treated with media containing 0.5% DMSO served as the untreated control. Cell viability was assessed using MTT dye (Invitrogen) in duplicate. Percent cell viability was calculated relative to the untreated control. All assays were performed in duplicate.

Recombinant IMPA1 expression and purification

Human IMPA1 was cloned into the pET28a plasmid at the *Nde*I and *Pst*I restriction sites. The recombinant protein was expressed in *Escherichia coli* BL21 (DE3) by culturing in 1 L of LB medium containing 50 µg/ml of kanamycin. The culture was incubated at 37 ℃ with 250 rpm shaking until the optical density at 600 nm reached 1.0. Protein expression was induced with 1 mM isopropyl β-D-thiogalactoside and the incubation continued at 20 ℃ with 200 rpm shanking for 20 h. The cells were harvested by centrifugation.

The cell pellets were resuspended in 20 mM sodium phosphate buffer (pH 7.4) containing 300 mM NaCl and 10 mM imidazole, then sonicated on ice for 5 min. The lysate was centrifuged at 12,500 rpm for 1 h to collect supernatant, which was then purified using immobilized metal affinity chromatography (TALON, Takara Bio, Japan). Unbound proteins were removed using 20 mM sodium phosphate buffer (pH 7.4), containing 300 mM NaCl and 20 mM imidazole. Elution of IMPA1 protein was carried out using 20 mM sodium phosphate buffer (pH 7.4) containing 300 mM NaCl and varying concentrations of imidazole (40, 100, 250, 400 mM). The eluted protein was dialyzed against 20 mM Tris-HCl pH 7.5 containing 10% glycerol at 4 ℃ for 8 h and stored at -20 °C until use.

In vitro enzymatic assays using recombinant IMPA1

The inhibitory effects of ebselen and lithium were assessed in a 20 µl reaction, following previously described protocols with minor modifications[17]. IMPA1 (5 ng) was incubated with various concentrations of ebselen (0–10 µM) and lithium (0–100 mM) for 30 min on ice. Subsequently, 1 mM of inositol monophosphate substrate and reaction mixture containing 50 mM Tris-HCl (pH 7.5), 1 mM ethylenediaminetetraacetic acid (EDTA), 3 mM $MgCl_2$, 150 mM KCl, 0.5 mg/mL bovine serum albumin (BSA) and 0.01% (v/v) Triton X-100 were added. The reaction was incubated at 37 ℃ for 1 h. Phosphate concentration was determined using a phosphate assay kit

(Abcam, UK), following manufacturer's protocols, and incubated for 30 min at RT in the dark. Absorbance at 595 nm was measured using a Sunrise absorbance reader (TECAN, Switzerland).

Cellular myo-inositol levels

Cells were seeded in 6-well plates at a density of 5×10^5 cells/well. The following day, cells were treated with 25 µM ebselen, 30 mM LiCl, or 0.2% DMSO as the untreated control for 48 h. Cells were washed three times with phosphate-buffer saline (PBS) and collected by trypsinization. After cell counting, they were centrifuged, and the PBS was removed Cells were lysed with ice-cold inositol assay buffer. Lysates were then centrifuged, and the obtained supernatants were used for *myo*-inositol quantification using the *myo*-inositol assay kit (ab252896, Abcam), following the manufacturer's protocol.

Evaluation of the antiviral activity of ebselen and L690330 against various RNA viruses

Vero or imHC cells were seeded in 96-well plates at a density of 2×10^4 cells/well. The following day, imHC cells were infected with DENV-2 or ZIKV at a multiplicity of infection (MOI) of 1. Vero cells were infected with CHIKV, EV71 or IAV at MOI of 0.0025, 0.02 and 1, respectively. Following the virus adsorption step, cells were maintained in 2% FBS media containing twofold serial dilutions of ebselen or L690,330 for 48 h, or for 24 h in the case of CHIKV infection. Medium containing 0.5% DMSO was used as the untreated control. Subsequently, viral supernatants were harvested and virus titers were determined. Percent inhibition was calculated relative to the virus titer of the infected untreated control. Each experiment was performed in triplicate.

IMPA1 silencing using SiRNA

imHC cells were seeded in a 24-well plate at a density of 6.5×10^4 cells/well. The following day, cells were transfected with 25 nM of siRNA targeting IMPA1 (si_IMPA1) from the ON-TARGETplus Human IMPA1 siRNA pool (Horizon Discovery, UK) using DharmaFECT™ Transfection Reagents (Horizon Discovery, UK), according to the manufacturer's protocol. Irrelevant siRNA (si_irrelevant) from the ON-TARGETplus non-targeting pool (D-001810-10-05, Horizon Discovery, UK) was transfected as a non-targeting control. Two days post-transfection, cells were either mock-infected or infected with DENV-2 at a MOI of 2 for 2 h. After removing the viral inoculum, cells were maintained in media containing either 20 µM ebselen or no ebselen for 1 day under both si_irrelevant and si_IMPA1 conditions. Viral supernatants were then collected for virus titer quantification, and cells were harvested for western blot analysis to assess the expression levels of IMPA1, DENV-2 NS1, and GAPDH, which served as an internal loading control.

Reversion of Ebselen antiviral activity by inositol or PI

imHC cells were inoculated with DENV-2 or ZIKV at an MOI of 1. Alternatively, Vero cells were inoculated with EV71, IAV, or CHIKV at MOIs of 0.02, 1, or 0.0025, respectively. After 2 h of viral inoculation, the inoculum was removed and cells were maintained in media containing various concentrations of ebselen, inositol, mixtures of ebselen and inositol, PI, or mixtures of ebselen and PI. Virus supernatants were collected at 24 h post-infection (hpi) for CHIKV, and at 48 hpi for DENV-2, ZIKV, EV71, and IAV, and were subjected to viral titer quantification.

Viral quantification

DENV-2 and ZIKV quantification by focus forming assay

The procedure was described elsewhere[35]. Briefly, Vero cells were seeded in 96-well plates at a density of 4×10^4 cells/well. The following day, cells were infected with 10-fold serially diluted virus supernatants for 2 h. Thereafter, cells were overlaid with overlay medium (1.5% carboxymethylcellulose in 2% FBS-MEM, with penicillin/streptomycin) and incubated at 37 °C with 5% CO_2 for 3 days for DENV-2 or 2 days for ZIKV. After incubation, the overlay medium was removed, and the cells were washed several times with PBS. Cells were then fixed with 3.7% (v/v) formaldehyde in PBS for 10 min at RT. Following fixation, cells were permeabilized using 2% (v/v) Triton-X-100/PBS for 10 min at RT, then washed with with PBS. The cells were probed with anti-flavivirus envelope protein antibody (4G2) and a 1:1000 dilution of alkaline phosphatase-conjugated goat anti-mouse IgG H + L (Invitrogen, 62–522) in 0.5% (v/v) Tween-20/PBS. Each antibody incubation was performed for 1 h at 37 °C, with three PBS washes between steps to remove excess antibody. Subsequently, the chromogenic substrate [100 mM Tris, pH 9.5, 100 mM NaCl, 5 mM $MgCl_2$, 0.335 mg/ml Nitroblue Tetrazolium (NDB0379, BioBasic), and 0.165 mg/ml BCIP-T (R0821, Thermo Scientific)] was added and incubated for 10 min at RT in the dark. Excess substrate was removed by washing with tap water. Foci were then counted, and virus titers were calculated as focus-forming units per ml (ffu/ml).

EV71 and CHIKV quantifications by plaque assay

Vero cells were seeded in 24-well plates at a density of 1.5×10^5 cells/well. The following day, cells were infected with 10-fold serially diluted EV71 or CHIKV virus supernatants for 2 h. Then, the inoculum was removed, and cells were overlaid with 1 ml of overlay medium (1.2% microcrystalline cellulose (Avicel, RC-591) in 2% FBS-MEM) and incubated at 37 °C with 5% CO_2 for 3 days for EV71 or 2 days for CHIKV. The overlay medium was removed, and the cells were fixed with 10% (v/v) formaldehyde in PBS for 1 h. Cells were stained with 1% (w/v) crystal violet in 20% (v/v) ethanol for 5 minutes and washed with tap water to remove excess dye. The plaques were counted and the virus titers were calculated as plaque-forming units per ml (pfu/ml).

Plaque assay for IAV

MDCK cells were seeded in 24-well plates at a density of 1.5×10^5 cells/well. The following day, cells were washed once with serum-free MEM containing 1 µg/ml of TPCK-treated trypsin (MEM + TPCK). Then, they were infected with 10-fold serial dilutions of viral samples in MEM + TPCK for 1.5 h. Subsequently, the inoculum was

discarded, and cells were overlaid with 1 ml of 1.2% microcrystalline cellulose (Avicel, RC-591) in MEM + TPCK, and incubated at 37 °C with 5% CO_2 for 2 days. The cells were fixed and stained as described earlier. The number of plaques was counted, and virus titers were determined as plaque-forming units per ml (pfu/ml).

Immunofluorescence assays

imHC cells were seeded in 24-well plates at a density of 7×10^4 cells/well with coverslips. The following day, cells were infected with ZIKV at MOI 1 for 2 h. After removal of the inoculum, cells were further cultivated in 2% FBS media containing ebselen or 0.5% DMSO as the untreated control. Then, cells were fixed with 4% (v/v) formaldehyde in PBS for 10 min at 4°C at 48 hpi. Subsequently, cells were permeabilized with 0.2% Triton-X-100 in PBS for 15 min at RT. Cells were probed with a 1:50 dilution of mouse anti-PI4P IgM (Z-P004, Echelon Biosciences) and a 1:1000 dilution of rabbit anti-ZIKV-NS1 IgG (GTX133306, Genetex) and incubated at 37 °C for 1 h. Then, cells were incubated with secondary antibody-conjugated fluorescence dyes and a 1:2000 dilution of Hoechst dye and incubated at 37 °C for 1 h. The images were taken using a confocal microscope.

Western blot analysis

After removing the media, cells were washed with PBS and lysed in RIPA buffer [50 mM Tris-HCl, pH 8.0; 150 mM NaCl; 0.1% Triton X-100; 0.5% sodium deoxycholate; 0.1% sodium dodecyl sulfate (SDS); 1 mM sodium orthovanadate; and 1 mM NaF]. Cell lysates were prepared by centrifugation at 12,000 × g for 10 min at 4 °C to remove debris. Protein concentrations were determined using the Bradford assay. Lysates (15 µg) were mixed with sample loading dye and reducing reagent, then loaded onto NuPAGE 4–12% Bis-Tris protein gels (1.0 mm; NP0322BOX, Thermo Fisher Scientific) and subjected to electrophoresis. Separated proteins were transferred onto nitrocellulose membranes (PALL). Membranes were blocked with 3% (w/v) skim milk in 0.1% (v/v) Tween-20/TBS for 1 h at room temperature, then probed overnight at 4 °C with continuous rocking using a 1:2000 dilution of rabbit anti-IMPA1 (AB184165, Abcam), a 1:2000 dilution of DENV-2-NS1 (PA5-32207, Thermo Scientific), or a 1:10,000 dilution of mouse anti-GAPDH (sc-47724, Santa Cruz Biotechnology). After washing, membranes were incubated for 2 h at room temperature with a 1:2000 dilution of HRP-conjugated goat anti-rabbit IgG or a 1:5000 dilution of HRP-conjugated rabbit anti-mouse IgG. Protein bands were visualized using Clarity Western ECL substrate (Bio-Rad Laboratories, Hercules, CA, USA) and imaged with ImageQuant LAS 4010 (GE Healthcare, Chicago, IL, USA). Band intensities were quantified using ImageJ software (U.S. National Institutes of Health, Bethesda, MD, USA) and normalized to GAPDH expression levels. The expression levels of IMPA1 and DENV-2 NS1 were presented as relative expression levels: IMPA1 was compared with untransfected cells, and DENV-2 NS1 was compared with cells not treated with ebselen.

Statistical analysis

An independent samples *t*-test was used to compare differences between two groups (untreated control vs. treated, or ebselen alone vs. ebselen combined with inositol or PI) using SPSS Statistics software (SPSS, Inc., Chicago, IL, USA); $p \leq 0.05$ was considered statistically significant. The 50% cytotoxic concentration (CC_{50}) and half-maximal inhibitory concentration (IC_{50}) values were calculated from dose-response curves of antiviral treatment by non-linear regression analysis using GraphPad Prism 10 (GraphPad Software, Inc., CA).

Data availability

All data generated or analyzed during this study are included in this published article (and its Supplementary Information files).

Received: 10 June 2025; Accepted: 11 November 2025
Published online: 29 December 2025

References

1. Helen Ifedilichukwu, N. H. & Joy, O. S. in *Antiviral Strategies in the Treatment of Human and Animal Viral Infections* (ed Arli Aditya Parikesit) (IntechOpen, 2023).
2. Schlicksup, C. J. & Zlotnick, A. Viral structural proteins as targets for antivirals. *Curr. Opin. Virol.* **45**, 43–50. https://doi.org/10.1016/j.coviro.2020.07.001 (2020).
3. Santi, C., Scimmi, C. & Sancineto, L. Ebselen and analogues: Pharmacological properties and synthetic strategies for their Preparation. *Molecules* **26**, 4230 (2021).
4. Amporndanai, K. et al. Inhibition mechanism of SARS-CoV-2 main protease by Ebselen and its derivatives. *Nat. Commun.* **12**, 3061. https://doi.org/10.1038/s41467-021-23313-7 (2021).
5. Qiao, Z. et al. The Mpro structure-based modifications of Ebselen derivatives for improved antiviral activity against SARS-CoV-2 virus. *Bioorg. Chem.* **117**, 105455. https://doi.org/10.1016/j.bioorg.2021.105455 (2021).
6. Zhang, H. et al. Identification of Ebselen derivatives as novel SARS-CoV-2 main protease inhibitors: Design, synthesis, biological evaluation, and structure-activity relationships exploration. *Bioorg. Med. Chem.* **96**, 117531. https://doi.org/10.1016/j.bmc.2023.117531 (2023).
7. Menéndez, C. A., Byléhn, F., Perez-Lemus, G. R., Alvarado, W. & de Pablo, J. J. Molecular characterization of Ebselen binding activity to SARS-CoV-2 main protease. *Sci. Adv.* **6**, eabd0345. https://doi.org/10.1126/sciadv.abd0345 (2020).
8. Jin, Z. et al. Structure of M(pro) from SARS-CoV-2 and discovery of its inhibitors. *Nature* **582**, 289–293. https://doi.org/10.1038/s41586-020-2223-y (2020).
9. Zmudzinski, M. et al. Ebselen derivatives inhibit SARS-CoV-2 replication by Inhibition of its essential proteins: PL(pro) and M(pro) proteases, and nsp14 guanine N7-methyltransferase. *Sci. Rep.* **13**, 9161. https://doi.org/10.1038/s41598-023-35907-w (2023).
10. Sahoo, P. et al. Detailed insights into the inhibitory mechanism of new Ebselen derivatives against main protease (Mpro) of severe acute respiratory syndrome Coronavirus-2 (SARS-CoV-2). *ACS Pharmacol. Translational Sci.* **6**, 171–180. https://doi.org/10.1021/acsptsci.2c00203 (2023).

11. Sinsulpsiri, S. et al. Unveiling the antiviral inhibitory activity of Ebselen and ebsulfur derivatives on SARS-CoV-2 using machine learning-based QSAR, LB-PaCS-MD, and experimental assay. *Sci. Rep.* **15**, 6956. https://doi.org/10.1038/s41598-025-91235-1 (2025).
12. Imprachim, N., Yosaatmadja, Y. & Newman, J. A. Crystal structures and fragment screening of SARS-CoV-2 NSP14 reveal details of exoribonuclease activation and mRNA capping and provide starting points for antiviral drug development. *Nucleic Acids Res.* **51**, 475–487. https://doi.org/10.1093/nar/gkac1207 (2023).
13. Thenin-Houssier, S. et al. Ebselen, a Small-Molecule capsid inhibitor of HIV-1 replication. *Antimicrob. Agents Chemother.* **60**, 2195–2208. https://doi.org/10.1128/aac.02574-15 (2016).
14. Chockalingam, K., Simeon, R. L., Rice, C. M. & Chen, Z. A cell protection screen reveals potent inhibitors of multiple stages of the hepatitis C virus life cycle. *Proc. Natl. Acad. Sci. U S A.* **107**, 3764–3769. https://doi.org/10.1073/pnas.0915117107 (2010).
15. Mukherjee, S. et al. Ebselen inhibits hepatitis C virus NS3 helicase binding to nucleic acid and prevents viral replication. *ACS Chem. Biol.* **9**, 2393–2403. https://doi.org/10.1021/cb500512z (2014).
16. Kraft, L., Roe, S. M., Gill, R. & Atack, J. R. Co-crystallization of human inositol monophosphatase with the lithium mimetic L-690,330. *Acta Crystallogr. D Struct. Biol.* **74**, 973–978. https://doi.org/10.1107/s2059798318010380 (2018).
17. Singh, N. et al. A safe lithium mimetic for bipolar disorder. *Nat. Commun.* **4**, 1332. https://doi.org/10.1038/ncomms2320 (2013).
18. Singh, N. et al. Effect of the putative lithium mimetic Ebselen on brain Myo-Inositol, Sleep, and emotional processing in humans. *Neuropsychopharmacology* **41**, 1768–1778. https://doi.org/10.1038/npp.2015.343 (2016).
19. Ramli, F. F., Cowen, P. J. & Godlewska, B. R. The potential use of Ebselen in Treatment-Resistant depression. *Pharmaceuticals* **15**, 485 (2022).
20. Sharpley, A. L. et al. A phase 2a randomised, double-blind, placebo-controlled, parallel-group, add-on clinical trial of Ebselen (SPI-1005) as a novel treatment for mania or hypomania. *Psychopharmacology* **237**, 3773–3782. https://doi.org/10.1007/s00213-020-05654-1 (2020).
21. Bizzarri, M., Monti, N., Piombarolo, A., Angeloni, A. & Verna, R. Myo-Inositol and D-Chiro-Inositol as modulators of ovary steroidogenesis: A narrative review. *Nutrients* **15**, 1875 (2023).
22. Axe, E. L. et al. Autophagosome formation from membrane compartments enriched in phosphatidylinositol 3-phosphate and dynamically connected to the Endoplasmic reticulum. *J. Cell. Biol.* **182**, 685–701. https://doi.org/10.1083/jcb.200803137 (2008).
23. Godi, A. et al. FAPPs control Golgi-to-cell-surface membrane traffic by binding to ARF and PtdIns(4)P. *Nat. Cell. Biol.* **6**, 393–404. https://doi.org/10.1038/ncb1119 (2004).
24. Beziau, A., Brand, D. & Piver, E. The role of phosphatidylinositol phosphate kinases during viral infection. *Viruses* **12**. https://doi.org/10.3390/v12101124 (2020).
25. Kutateladze, T. G. Translation of the phosphoinositide code by PI effectors. *Nat. Chem. Biol.* **6**, 507–513. https://doi.org/10.1038/nchembio.390 (2010).
26. Delang, L., Paeshuyse, J. & Neyts, J. The role of phosphatidylinositol 4-kinases and phosphatidylinositol 4-phosphate during viral replication. *Biochem. Pharmacol.* **84**, 1400–1408. https://doi.org/10.1016/j.bcp.2012.07.034 (2012).
27. Shears, B. S. The versatility of inositol phosphates as cellular signals. *Biochim. Et Biophys. Acta (BBA) - Mol. Cell. Biology Lipids.* **1436**, 49–67. https://doi.org/10.1016/S0005-2760(98)00131-3 (1998).
28. Su, X. B., Ko, A. A. & Saiardi, A. Regulations of myo-inositol homeostasis: Mechanisms, implications, and perspectives. *Adv. Biol. Regul.* **87**, 100921. https://doi.org/10.1016/j.jbior.2022.100921 (2023).
29. De Craene, J. O., Bertazzi, D. L., Bär, S., Friant, S. & Phosphoinositides major actors in membrane trafficking and lipid signaling pathways. *Int. J. Mol. Sci.* **18**. https://doi.org/10.3390/ijms18030634 (2017).
30. Schneider, S. Inositol transport proteins. *FEBS Lett.* **589**, 1049–1058. https://doi.org/10.1016/j.febslet.2015.03.012 (2015).
31. Tu-Sekine, B. & Kim, S. F. The inositol phosphate System-A coordinator of metabolic adaptability. *Int. J. Mol. Sci.* **23**. https://doi.org/10.3390/ijms23126747 (2022).
32. Chen, Q., Shen, L. & Li, S. Emerging role of inositol monophosphatase in cancer. *Biomed. Pharmacother.* **161**, 114442. https://doi.org/10.1016/j.biopha.2023.114442 (2023).
33. Li, H. et al. Targeting PI3K family with small-molecule inhibitors in cancer therapy: current clinical status and future directions. *Mol. Cancer.* **23**, 164. https://doi.org/10.1186/s12943-024-02072-1 (2024).
34. Altan-Bonnet, N. & Balla, T. Phosphatidylinositol 4-kinases: hostages Harnessed to build panviral replication platforms. *Trends Biochem. Sci.* **37**, 293–302. https://doi.org/10.1016/j.tibs.2012.03.004 (2012).
35. Jitobaom, K. et al. Identification of inositol monophosphatase as a broad-spectrum antiviral target of Ivermectin. *J. Med. Virol.* **96**, e29552. https://doi.org/10.1002/jmv.29552 (2024).
36. Ci, Y., Yang, Y., Xu, C., Qin, C. F. & Shi, L. Electrostatic interaction between NS1 and negatively charged lipids contributes to flavivirus replication organelles formation. *Front. Microbiol.* **12**. https://doi.org/10.3389/fmicb.2021.641059 (2021).
37. Oostwoud, L. C. et al. Apocynin and Ebselen reduce influenza A virus-induced lung inflammation in cigarette smoke-exposed mice. *Sci. Rep.* **6**, 20983. https://doi.org/10.1038/srep20983 (2016).
38. Haddad, E. B. et al. Differential effects of Ebselen on neutrophil Recruitment, Chemokine, and inflammatory mediator expression in a rat model of Lipopolysaccharide-Induced pulmonary inflammation. *J. Immunol.* **169**, 974–982. https://doi.org/10.4049/jimmunol.169.2.974 (2002).
39. Belvisi, M. G. et al. Anti-inflammatory properties of Ebselen in a model of sephadex-induced lung inflammation. *Eur. Respir J.* **15**, 579–581. https://doi.org/10.1034/j.1399-3003.2000.15.25.x (2000).
40. Govero, J. et al. Zika virus infection damages the testes in mice. *Nature* **540**, 438–442. https://doi.org/10.1038/nature20556 (2016).
41. Simanjuntak, Y. et al. Ebselen alleviates testicular pathology in mice with Zika virus infection and prevents its sexual transmission. *PLoS Pathog.* **14**, e1006854. https://doi.org/10.1371/journal.ppat.1006854 (2018).
42. Giurg, M. et al. Reaction of bis[(2-chlorocarbonyl)phenyl] diselenide with Phenols, Aminophenols, and other amines towards Diphenyl diselenides with antimicrobial and antiviral properties. *Molecules* **22**, 974 (2017).
43. Zhao, Y. et al. Lithium chloride confers protection against viral myocarditis via suppression of coxsackievirus B3 virus replication. *Microb. Pathog.* **144**, 104169. https://doi.org/10.1016/j.micpath.2020.104169 (2020).
44. Qaswal, A. B., Suleiman, A., Guzu, H., Harb, T. & Atiyat, B. The potential role of lithium as an antiviral agent against SARS-CoV-2 via membrane depolarization: review and hypothesis. *Sci. Pharm.* **89**, 11 (2021).
45. Harrison, S. M., Tarpey, I., Rothwell, L., Kaiser, P. & Hiscox, J. A. Lithium chloride inhibits the coronavirus infectious bronchitis virus in cell culture. *Avian Pathol.* **36**, 109–114. https://doi.org/10.1080/03079450601156083 (2007).
46. Cui, J. et al. Inhibitory effects of lithium chloride on replication of type II Porcine reproductive and respiratory syndrome virus in vitro. *Antivir. Ther.* **20**, 565–572. https://doi.org/10.3851/imp2924 (2015).
47. Puertas, M. C. et al. Effect of lithium on HIV-1 expression and proviral reservoir size in the CD4 + T cells of antiretroviral therapy suppressed patients. *Aids* **28**, 2157–2159. https://doi.org/10.1097/qad.0000000000000374 (2014).
48. Amsterdam, J. D., Maislin, G. & Rybakowski, J. A possible antiviral action of lithium carbonate in herpes simplex virus infections. *Biol. Psychiatry.* **27**, 447–453. https://doi.org/10.1016/0006-3223(90)90555-g (1990).
49. Atack, J. R., Cook, S. M., Watt, A. P., Fletcher, S. R. & Ragan, C. I. In vitro and in vivo Inhibition of inositol monophosphatase by the bisphosphonate L-690,330. *J. Neurochem.* **60**, 652–658. https://doi.org/10.1111/j.1471-4159.1993.tb03197.x (1993).
50. Atack, J. R., Rapoport, S. I. & Varley, C. L. Characterization of inositol monophosphatase in human cerebrospinal fluid. *Brain Res.* **613**, 305–308. https://doi.org/10.1016/0006-8993(93)90916-B (1993).

51. Rogers, M. J. et al. Cellular and molecular mechanisms of action of bisphosphonates. *Cancer* **88**, 2961–2978. https://doi.org/10.1002/1097-0142(20000615)88:12+<2961::AID-CNCR12>3.0.CO;2-L (2000).
52. Zielińska, M. et al. Determination of bisphosphonate properties in terms of bioavailability, bone affinity, and cytotoxicity. *Pharmacol. Rep.* **76**, 1160–1173. https://doi.org/10.1007/s43440-024-00624-2 (2024).
53. Atack, J. R. et al. Effects of L-690,488, a prodrug of the bisphosphonate inositol monophosphatase inhibitor L-690,330, on phosphatidylinositol cycle markers. *J. Pharmacol. Exp. Ther.* **270**, 70–76. https://doi.org/10.1016/S0022-3565(25)22382-5 (1994).
54. Grazia Martina, M. et al. Bithiazole inhibitors of phosphatidylinositol 4-kinase (PI4KIIIβ) as broad-spectrum antivirals blocking the replication of SARS-CoV-2, Zika virus, and human rhinoviruses. *ChemMedChem* 16, 3548–3552. https://doi.org/10.1002/cmdc.202100483 (2021).
55. Azad, G. K. & Tomar, R. S. Ebselen, a promising antioxidant drug: mechanisms of action and targets of biological pathways. *Mol. Biol. Rep.* **41**, 4865–4879. https://doi.org/10.1007/s11033-014-3417-x (2014).
56. Dangsagul, W. et al. Zika virus isolation, propagation, and quantification using multiple methods. *PLoS One*. **16**, e0255314. https://doi.org/10.1371/journal.pone.0255314 (2021).
57. Noisumdaeng, P. et al. Complete genome analysis demonstrates multiple introductions of enterovirus 71 and coxsackievirus A16 recombinant strains into Thailand during the past decade. *Emerg. Microbes Infect.* **7**, 214. (2018). https://doi.org/10.1038/s41426-018-0215-x

Acknowledgements

We are grateful to Miss Pucharee Songprakhon for her assistance with confocal microscopy analysis.

Author contributions

KJ performed drug treatments, confocal microscopy analysis, myo-inositol and phosphate quantifications, preparing figures, and writing manuscripts. UB performed and wrote the methodology for *in vitro* enzymatic assay and edited the manuscript. CB was responsible for project administration, prepared chemicals and viral stock. TS prepared viral stocks. PA supervised the study project, wrote and edited the manuscript, and acquired funding. All authors approved the submitted version.

Funding

This study was supported by the National Research Council of Thailand (NRCT) under grant number N42A670585. Partial support was also provided by the Faculty of Medicine Siriraj Hospital, Mahidol University, Thailand.

Declarations

Competing interests

The authors declare no competing interests.

Ethical approval

This study was approved by Faculty of Medicine Siriraj Hospital Biosafety Committee (approval no. SI 2024-015). All experiments involving infectious viruses were performed in BSL-2 laboratory.

Additional information

Supplementary Information The online version contains supplementary material available at https://doi.org/10.1038/s41598-025-28652-9.

Correspondence and requests for materials should be addressed to P.A.